



Cite this: *Phys. Chem. Chem. Phys.*,  
2016, **18**, 23304

# Concentric dual $\pi$ aromaticity in bowl-like $B_{30}$ cluster: an all-boron analogue of corannulene†

Kang Wang,<sup>a</sup> Da-Zhi Li,<sup>\*b</sup> Rui Li,<sup>a</sup> Lin-Yan Feng,<sup>a</sup> Ying-Jin Wang<sup>a</sup> and  
Hua-Jin Zhai<sup>\*a,c</sup>

A chemical bonding model is presented for the bowl-like  $C_{5v}$   $B_{30}$  global-minimum cluster with a central pentagonal hole. The  $B_{30}$  cluster is composed of three concentric boron rings: first  $B_5$ , second  $B_{10}$ , and third  $B_{15}$ . The first and second B rings constitute an inner double-chain ribbon and support a delocalized  $\pi$  sextet. The second and third rings form an outer double-chain ribbon, where  $14\pi$  delocalized electrons are situated. The unique  $\pi$  systems lead to concentric dual  $\pi$  aromaticity for  $B_{30}$ , a concept established from concerted computational data on the bases of canonical molecular orbital (CMO) analysis, adaptive natural density partitioning (AdNDP), nucleus-independent chemical shifts (NICS), and natural charge calculations. A proposal is put forward that the bowl-like  $B_{30}$  cluster is an exact all-boron analogue of corannulene ( $C_{20}H_{10}$ ), a fragment of  $C_{60}$  fullerene. The bonding nature of corannulene is revisited and fully elucidated herein. A comparison of the bonding patterns in bowl-like  $C_{5v}$   $B_{30}$  cluster and two other structural isomers ( $C_s$  and  $C_1$ ) unravels the mechanism as to why the defective hole prefers to be positioned at the center.

Received 25th June 2016,  
Accepted 30th July 2016

DOI: 10.1039/c6cp04464f

www.rsc.org/pccp

## 1. Introduction

During the past decade, elemental boron clusters have been of great interest in physical chemistry, materials science, and nanoscience and nanotechnologies. Boron clusters possess unusual structural and electronic properties and chemical bonding,<sup>1–29</sup> primarily owing to the intrinsic electron-deficiency of the element. Combined theoretical and experimental studies firmly establish a two-dimensional (2D) flatland of boron clusters, which is in sharp contrast to bulk boron or boron-based alloys. In the flatland, boron clusters were revealed to favor planar or quasi-planar structures as global minima at least up to  $B_{28}^-$  in the anions,<sup>7–26,30</sup>  $B_{20}$  in the neutral clusters,<sup>17</sup> and  $B_{16}^+$  in the cations.<sup>3</sup> Very recent work showed that beyond  $B_{28}^-$ , the  $B_{30}^-$ ,  $B_{35}^-$ , and  $B_{36}^-$  clusters,<sup>22,24–26</sup> as well as  $B_{40}^-$ ,<sup>27</sup> all possess quasi-planar structures with vacancies such as hexagons and

twin-hexagons, lending indirect experimental evidence for the viability of 2D atomic-thin boron sheets, or borophenes.<sup>25</sup> The observation of the first free-standing cage-like all-boron fullerenes or borospherenes,  $D_{2d}$   $B_{40}^{-10}$ , marks the genesis of borospherene chemistry.<sup>27</sup> Axially chiral  $C_3/C_2$   $B_{39}^-$  borospherene<sup>28</sup> quickly followed, which is the first borospherene anion as the global minimum. Subsequently, new chiral members were introduced to the borospherene family:  $C_1$   $B_{41}^+$  and  $C_2$   $B_{42}^{2+}$ .<sup>29</sup> The structures and bonding in borospherenes feature interwoven boron double chains and  $\pi$  plus  $\sigma$  double delocalization, which compensate for boron's electron-deficiency.<sup>27</sup>

Two general concepts appear to dominate the chemical bonding in 2D boron: ( $\pi$  and  $\sigma$ ) aromaticity/antiaromaticity and hydrocarbon analogy,<sup>5,6</sup> the latter including polycyclic aromatic hydrocarbons (PAHs). Notably, the series of  $B_8^{2-}$ ,  $B_9^-$ ,  $B_{10}$ ,  $B_{11}^-$ ,  $B_{12}$ , and  $B_{13}^+$  clusters were shown to possess  $6\pi$  electrons, following the  $(4n + 2)$  Hückel rule for aromaticity. These clusters are considered as inorganic, all-boron analogues of benzene.<sup>5,6,12</sup> For the binary B–O and B–S systems, the  $B_6O_6$  cluster<sup>31</sup> (that is, the so-called boronyl<sup>32–35</sup> boroxine) with a  $B_3O_3$  boroxol ring was revealed as an analogue of benzene or boroxine  $B_3O_3H_3$ , whereas the  $B_6S_6^{0/-2-}$  clusters<sup>36</sup> with fused, twin  $B_3S_2$  rings were proposed to be analogues of naphthalene ( $C_{10}H_8$ ). Furthermore, the  $B_{16}^{2-}$ ,  $B_{22}^-$ , and  $B_{23}^-$  clusters were shown to be all-boron analogues of naphthalene, anthracene, and phenanthrene, respectively.<sup>14,19</sup> Remarkably, the  $B_{19}^-$  cluster was found to possess a nearly circular spider-web-like structure with a filled-pentagon  $B_6$  central unit and a 13-atom outer ring.<sup>16</sup>

<sup>a</sup> Nanocluster Laboratory, Institute of Molecular Science, Shanxi University, Taiyuan 030006, China. E-mail: hj.zhai@sxu.edu.cn

<sup>b</sup> Department of Chemical Engineering, Binzhou University, Binzhou 256603, China. E-mail: ldz005@126.com

<sup>c</sup> State Key Laboratory of Quantum Optics and Quantum Optics Devices, Shanxi University, Taiyuan 030006, China

† Electronic supplementary information (ESI) available: Comparison of the  $\pi$  canonical molecular orbitals (CMOs) of the bowl-like  $B_{30}$   $C_{5v}$  ( $^1A_1$ ) cluster and corannulene (Fig. S1); the charge distributions of  $B_{30}$   $C_{5v}$  ( $^1A_1$ ) and corannulene via natural bond orbital (NBO) calculations (Fig. S2); and the  $\pi$  CMOs of two representative local minima of the  $B_{30}$  cluster with the hole being situated off-center (Fig. S3). See DOI: 10.1039/c6cp04464f

It is doubly  $\pi$  aromatic, consisting of two concentric  $\pi$  systems, analogous to coronene ( $C_{24}H_{12}$ ). The structure and bonding of  $B_{19}^-$  immediately inspired the proposal of a molecular Wankel motor, because the inner  $B_6$  unit rotates within the peripheral  $B_{13}$  ring with a negligible rotation barrier.<sup>37</sup> A similar fluxional behavior was also found subsequently in the  $B_{13}^+$  cluster for its internal  $B_3$  triangle,<sup>38</sup> as well as in subnanoscale tank treads ( $B_{11}^-/B_{11}$  and  $B_{15}^+$ ).<sup>39,40</sup> For even larger 2D boron clusters, the  $C_{6v}$   $B_{36}$  cluster<sup>26</sup> was established to be a perfect all-boron analogue of coronene.

Nguyen and coworkers<sup>41</sup> recently reported a computational study on the  $B_{30}$  cluster, suggesting that it has a bowl-like global-minimum structure. It has a pentagonal  $B_5$  ring as the structural core and is successively built up by adding two strings of 10 and 15 boron atoms, respectively, to the core. The overall structure has  $C_{5v}$  symmetry, whose stability was accounted for using the concept of “disk-aromaticity”.<sup>41</sup> This unique, highly symmetric cluster invites further theoretical studies to elucidate its nature of bonding (for both the  $\sigma$  and  $\pi$  frameworks), as well as to address why the pentagonal hole is situated at the center of the bowl and how this cluster is relevant to the known hydrocarbons or PAHs. These issues are the focus of the present study.

In this contribution, we report a computational study on the structural and electronic properties and chemical bonding of the bowl-like  $B_{30}$  (**1**,  $C_{5v}$ ,  $^1A_1$ ) global-minimum cluster, unraveling two concentric  $\pi$  aromatic systems in the species. To be specific, the first  $B_5$  and second  $B_{10}$  rings constitute the inner circular ribbon of the cluster, which supports  $6\pi$  delocalized electrons. Similarly, the second  $B_{10}$  and third  $B_{15}$  rings form the outer ribbon, where  $14\pi$  electrons are situated. Concentric dual  $\pi$  aromaticity in  $B_{30}$  renders it an exact all-boron analogue of corannulene,  $C_{20}H_{10}$  (**2**,  $C_{5v}$ ,  $^1A_1$ ), whose nature of bonding is revisited and thoroughly elucidated herein. Aided by two isomeric structures,  $C_s$  and  $C_1$ , we also attempted to understand why the pentagonal hole in  $B_{30}$  prefers to be situated at the bowl center. We believe the present bonding concepts and analyses may be applicable to additional boron nanosystems.

## 2. Computational methods

Structural optimizations of the  $B_{30}$  cluster and corannulene were carried out using density-functional theory (DFT) at the PBE0/6-311+G(d) level,<sup>42–45</sup> starting from an initial structure based on the literature for the  $B_{30}$  global minimum.<sup>41</sup> Two other isomeric structures were also searched and optimized for  $B_{30}$ , which differ from the global minimum in terms of the position of the defective hole. The PBE0 level of theory has been benchmarked lately as a reliable DFT method for boron clusters.<sup>46,47</sup>

Chemical bonding in the  $B_{30}$  and corannulene systems was first analyzed on the basis of  $\pi$  canonical molecular orbitals (CMOs). Alternatively, adaptive natural density partitioning (AdNDP)<sup>48</sup> analysis was performed, which enables an understanding of the bonding for all valence electrons, both  $\sigma$  and  $\pi$ . Since the AdNDP method is not sensitive to the level of theory or the basis sets used, we chose to carry out AdNDP calculations

at the PBE0/6-31G level. To assess the nature of aromaticity in the systems, nucleus-independent chemical shifts (NICS)<sup>49</sup> were calculated. Natural bond orbital (NBO) analysis<sup>50</sup> was carried out to obtain the natural atomic charges and Wiberg bond indices (WBI).

The AdNDP analysis was performed using the AdNDP program.<sup>48</sup> All other calculations and analyses were performed using the Gaussian 09 software package.<sup>51</sup> The visualization of AdNDP results was realized using the Molekel program.<sup>52</sup>

## 3. Results and discussion

### 3.1. Bowl-like $B_{30}$ cluster: structure, $\pi$ bonding, and analogy to corannulene

The optimized global-minimum structure of  $B_{30}$  (**1**,  $C_{5v}$ ,  $^1A_1$ ) at the PBE0/6-311+G(d) level is depicted in Fig. 1(a). Similar to a prior report,<sup>41</sup> the  $B_{30}$  (**1**) cluster possesses a circular, bowl-like structure with  $C_{5v}$  symmetry, which is composed of a pentagonal base and successively built up by adding two boron rings of 10 and 15 atoms. For the purpose of clarity, in the following these concentric building units are referred to as the first, second, and third B rings, respectively. The bowl shape and  $C_{5v}$  symmetry of  $B_{30}$  are reminiscent of a PAH species, corannulene  $C_{20}H_{10}$  (**2**,  $C_{5v}$ ,  $^1A_1$ ), whose reoptimized structure is depicted in Fig. 1(b). Corannulene, first synthesized by Barth and Lawton in 1966,<sup>53</sup> can be considered as a fragment of the celebrated  $C_{60}$  fullerene with the peripheral atoms being saturated by hydrogen. With  $C_{5v}$  symmetry, corannulene has four types of C–C bonds: rim, flank, spoke, and hub. One may attempt to understand their bond distances in terms of classical resonance structures.<sup>54,55</sup> In the  $C_5$  base, it has a mean C–C distance of 1.41 Å and a  $\angle$  CCC bond angle of  $108^\circ$ . The bowl depth is calculated to be 0.88 Å. According to the latest recommended covalent radii by Pyykkö,<sup>56,57</sup> the upper bound for C=C and C–C bonds should be 1.34 and 1.50 Å, respectively, and the C–C bond in the  $C_5$  base of **2** is between single and double bonds, hinting at a delocalized  $\pi$  system. The calculated WBI for C–C is 1.18, in line with the bond distance.

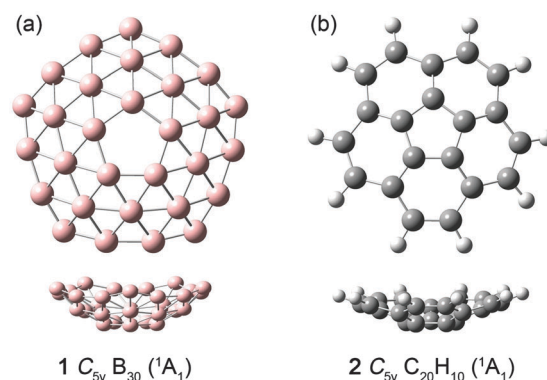


Fig. 1 Optimized structures of (a) the  $C_{5v}$  (**1**,  $^1A_1$ ) global minimum of  $B_{30}$  and (b)  $C_{5v}$  (**2**,  $^1A_1$ ) of  $C_{20}H_{10}$  at the PBE0/6-311+G(d) level. Both top and side views are shown. The B, C, and H atoms are in pink, thick gray, and light gray, respectively.

In terms of bonding in bowl-like B<sub>30</sub> (**1**), a B single ring is electron-deficient and unstable. Thus, the first and second B rings combine to form an inner B double-chain ribbon with 15 atoms (Fig. 1(a)), whereas the second and third B rings constitute an outer B ribbon with 25 atoms. The inner and outer B ribbons are circular and concentric, on which the delocalized  $\sigma$ - and  $\pi$ -bonds are situated (see below). The dimensions of the B<sub>30</sub> bowl are 7.46 Å in length, 7.47 Å in width, and 2.17 Å in height at the PBE0/6-311+G(d) level. The B–B distance within the pentagonal hole is calculated to be 1.66 Å, comparable to a typical single bond.<sup>35,57</sup> The B atoms in B<sub>30</sub> (**1**) have distinct coordination environments: (i) for the third B<sub>15</sub> ring, the 5 apex atoms are tricoordinated and the 10 edge atoms are tetracoordinated; (ii) the first B<sub>5</sub> ring shows penta-coordination; and (iii) the second B<sub>10</sub> ring features hexa-coordination. Thus, every B atom in this system is electron deficient, in particular those in the second B<sub>10</sub> ring.

The bowl-type quasi-planarity in B<sub>30</sub> (**1**, C<sub>5v</sub>) and corannulene C<sub>20</sub>H<sub>10</sub> (**2**, C<sub>5v</sub>) is relatively easy to rationalize. Corannulene is known to be a precursor for the C<sub>60</sub> buckyball, in which the pentagon is the key structural unit to facilitate the curvature of the surface. Therefore, the presence of a pentagon in corannulene naturally leads to its bowl shape and C<sub>5v</sub> symmetry. A similar argument applies for B<sub>30</sub> (**1**, C<sub>5v</sub>) in light of the chemical analogy between **1** and **2**. We stress that “quasi-planarity” is the norm for boron clusters,<sup>1–30</sup> because for a boron cluster the peripheral B–B link has a two-center two-electron (2c-2e)  $\sigma$  bond, which is further reinforced by delocalized  $\sigma$ - and  $\pi$ -bonding. For those encircled inside, the B–B distances are typically longer due to the occurrence of delocalized  $\sigma$ - and  $\pi$ -bonding only. Thus a “fastened” peripheral ring usually does not have enough space to accommodate the inner portion in a perfectly planar configuration, resulting in quasi-planar boron clusters. In our calculations, we confirmed that both the flattened structures of B<sub>30</sub> and C<sub>20</sub>H<sub>10</sub> have C<sub>2v</sub> symmetry, showing five and one imaginary frequency(ies), respectively. The C<sub>2v</sub> structures are 6.56 and 0.24 eV above the global minima for B<sub>30</sub> and C<sub>20</sub>H<sub>10</sub>, respectively, and the lowest imaginary frequencies for both structures correspond to the inversion mode. Alternatively, the origin of quasi-planarity in B<sub>30</sub> and C<sub>20</sub>H<sub>10</sub> may be investigated using the method proposed by Datta and coworkers,<sup>58,59</sup> which involves vibrational coupling between the relevant occupied CMOs and unoccupied CMOs.

To shed light on the bonding that underlies the bowl shape of B<sub>30</sub> (**1**, C<sub>5v</sub>, <sup>1</sup>A<sub>1</sub>), it is straightforward to plot the  $\pi$  CMOs in the system, as shown in Fig. S1(a) in the ESI†. A total of ten  $\pi$  CMOs are revealed, of which the HOMO–4 (where HOMO denotes the highest occupied molecular orbital), HOMO–1, and HOMO–1' involve the primary contributions from the inner B ribbon, whereas the remaining 7 CMOs are largely situated on the outer B ribbon (except HOMO–13, HOMO–12, and HOMO–12', which contain a component from the inner B ribbon as well). This  $\pi$  bonding pattern and  $\pi$  electron-counting turn out to be identical to those of C<sub>20</sub>H<sub>10</sub> (**2**, C<sub>5v</sub>, <sup>1</sup>A<sub>1</sub>) (Fig. S1(b), ESI†), suggesting that C<sub>5v</sub> B<sub>30</sub> (**1**) is an all-boron analogue of corannulene, in line with their structural similarity (Fig. 1). A similar comparison of the  $\sigma$  framework in B<sub>30</sub> (**1**, C<sub>5v</sub>)

and C<sub>20</sub>H<sub>10</sub> (**2**, C<sub>5v</sub>) is technically possible, in principle, which is beyond the focus of the present study.<sup>60</sup>

### 3.2. Adaptive natural density partitioning (AdNDP) analyses uncover the concentric dual $\pi$ aromaticity in the bowl-like B<sub>30</sub> cluster and corannulene

The  $\pi$  CMOs (Fig. S1, ESI†) as discussed above already suggest that the bonding in B<sub>30</sub> (**1**, C<sub>5v</sub>, <sup>1</sup>A<sub>1</sub>) and C<sub>20</sub>H<sub>10</sub> (**2**, C<sub>5v</sub>, <sup>1</sup>A<sub>1</sub>) has two concentric subsystems. For an in-depth understanding of the bonding nature in B<sub>30</sub> (**1**) and C<sub>20</sub>H<sub>10</sub> (**2**), it is helpful to perform AdNDP analyses,<sup>48</sup> which include both the  $\pi$  and  $\sigma$  frameworks and all valence electrons in the systems. As an extension of the NBO analysis, AdNDP represents the electronic structure of a molecule in terms of  $n$ -center two-electron ( $nc$ -2e) bonds, with  $n$  ranging from one to the total number of atoms in the molecule. Thus, the AdNDP analysis recovers the classical Lewis bonding elements (lone pairs and conventional 2c-2e bonds), as well as the nonclassical, delocalized  $nc$ -2e bonds.

Fig. 2 illustrates the AdNDP bonding patterns of C<sub>5v</sub> B<sub>30</sub> (**1**) and C<sub>5v</sub> C<sub>20</sub>H<sub>10</sub> (**2**). The B<sub>30</sub> cluster has a total of 90 valence electrons. Among them, 30 electrons are used for 15 classical 2c-2e  $\sigma$  bonds along the third B<sub>15</sub> ring (Fig. 2(a)). The remaining 60 electrons are delocalized in the  $\sigma$  and  $\pi$  frameworks. The delocalized  $\sigma$  framework contains 40 electrons (Fig. 2(a), first row), including five 3c-2e and five 4c-2e  $\sigma$  bonds in the inner B ribbon and ten 4c-2e  $\sigma$  bonds in the outer B ribbon. The twenty 3c-2e/4c-2e  $\sigma$  bonds cover the inner and outer ribbons almost uniformly,<sup>61</sup> further fastened by fifteen 2c-2e  $\sigma$  bonds along the third, peripheral B<sub>15</sub> ring. Overall, the  $\sigma$  framework in B<sub>30</sub> is robust, consuming 70 electrons.<sup>60</sup>

For the  $\pi$  framework in B<sub>30</sub> (**1**), 10 delocalized bonds are readily revealed (Fig. 2(a), third and fourth rows), which can be qualitatively traced back to the 10 CMOs in Fig. S1(a) (ESI†). Instructively, through the linear combination of  $\pi$  CMOs, the inner *versus* outer  $\pi$  subsystems are vividly unraveled in AdNDP, showing three 15c-2e  $\pi$  bonds in the inner B ribbon and seven 25c-2e  $\pi$  bonds in the outer one. Thus the ten  $\pi$  bonds in B<sub>30</sub> are clearly divided into two subsets, whose electron counts (6 $\pi$  for the inner ribbon *versus* 14 $\pi$  for the outer ribbon) conform to the (4*n* + 2) Hückel rule for aromaticity. The concentric dual  $\pi$  aromaticity<sup>16</sup> for the B<sub>30</sub> bowl is commensurate with its highly symmetric C<sub>5v</sub> structure. A schematic presentation of  $\pi$  bonding in C<sub>5v</sub> B<sub>30</sub> (**1**) is shown in Fig. 3(a).

A rhombic 4c-2e bond (and to a less extent, a 3c-2e or 5c-2e bond) in the double-chain B ribbons, either  $\pi$  or  $\sigma$ , is basically analogous to a 2c-2e C–C bond in hydrocarbons.<sup>47,62,63</sup> This conceptual link hints that corannulene, C<sub>5v</sub> C<sub>20</sub>H<sub>10</sub> (**2**), should possess a similar AdNDP pattern. As shown in Fig. 2(b), the  $\sigma$  framework of corannulene has ten C–H, fifteen peripheral (rim and flank) C–C, five spoke C–C, and five hub C–C  $\sigma$  bonds. All these 35  $\sigma$  bonds are 2c-2e in nature. For the  $\pi$  framework, the inner subset consists of three 10c-2e  $\pi$  bonds and the outer has seven 15c-2e  $\pi$  bonds, which are similar to the concentric dual  $\pi$  aromatic pattern in C<sub>5v</sub> B<sub>30</sub> (**1**). The essence of  $\pi$  bonding in corannulene is summarized in Fig. 3(b). It should be stressed that the inner  $\pi$  system needs to be expanded to 10c-2e  $\pi$  bonds, rather than just 5c-2e  $\pi$  bonds. The latter option has occupation numbers (ONs) of as low as 1.39 |*e*| (Fig. 4), which are less than ideal.

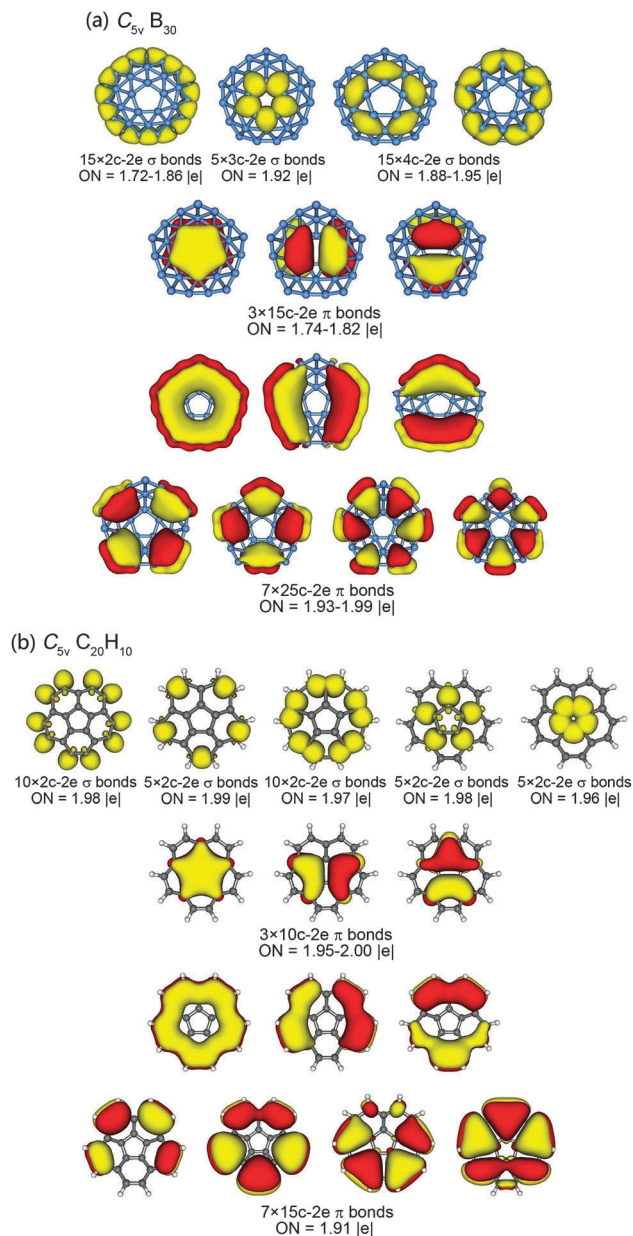


Fig. 2 Chemical bonding patterns for (a)  $C_{5v} B_{30}$  (**1**,  $^1A_1$ ) and (b)  $C_{5v} C_{20}H_{10}$  (**2**,  $^1A_1$ ), as revealed for the adaptive natural density partitioning (AdNDP) analyses. Occupation numbers (ONs) are indicated, where an ON value of 2.0 |e| represents an ideal case.

The electron-counting mechanism also underlies this expansion. Indeed, while not being exact (see below), corannulene has long been viewed as the fusion of two charged concentric conjugated systems: an inner cyclopentadienyl anion and an outer [15]annulene cation.<sup>53</sup> The spoke C–C units should thus participate partially in the inner  $\pi$  system in order to fulfill the  $\pi$  sextet in the hub.

### 3.3. Nucleus independent chemical shifts, natural charges, and the bonding of corannulene revisited

NICS calculations offer an independent theoretical measure of aromaticity. The bowl-like  $C_{5v} B_{30}$  (**1**) cluster has a negative NICS<sub>zz</sub>(1) of  $-57.9$  ppm, calculated at 1 Å above the bowl center.

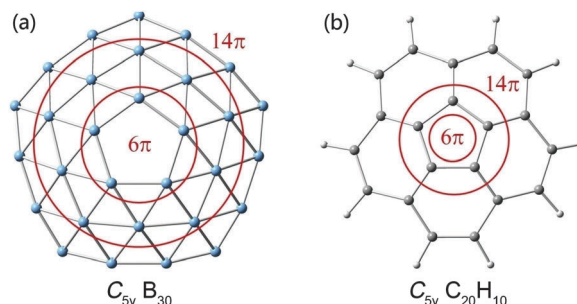


Fig. 3 Schematic presentations of the essence of  $\pi$  bonding in (a)  $C_{5v} B_{30}$  (**1**,  $^1A_1$ ) and (b)  $C_{5v} C_{20}H_{10}$  (**2**,  $^1A_1$ ). The species possess concentric dual  $\pi$  aromaticity, featuring 6 $\pi$  electrons for the inner circle and 14 $\pi$  electrons for the outer circle.

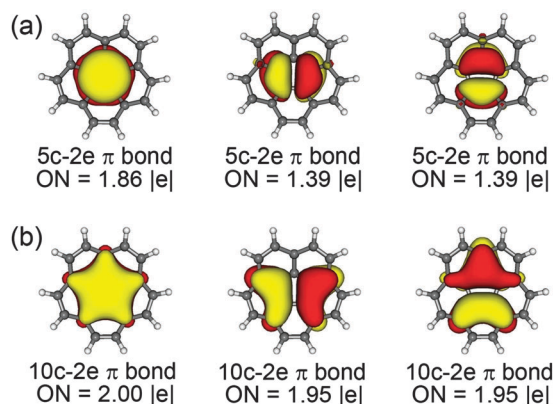


Fig. 4 The adaptive natural density partitioning (AdNDP) bonding patterns for the inner  $\pi$  sextet in  $C_{5v} C_{20}H_{10}$  (**2**,  $^1A_1$ ). The values of the occupation number (ON) increase markedly from the (a) 5c-2e to (b) 10c-2e cases. The 5c-2e option is consistent with 5 $\pi$  electrons only, whereas the 10c-2e option offers a perfect  $\pi$  sextet, indicating that the five spoke C sites collectively contribute one electron to the inner  $\pi$  system.

This value indicates that **1** is highly  $\pi$  aromatic, consistent with the nature of concentric dual  $\pi$  aromaticity and the 6 $\pi$  versus 14 $\pi$  electron counts. In comparison, the prototypical  $\pi$  aromatic hydrocarbon, benzene ( $C_6H_6$ ), has a calculated NICS<sub>zz</sub>(1) value of  $-27.9$  ppm. We note that NICS as a criterion for aromaticity fails completely<sup>64</sup> for the pentagonal hole in corannulene, with a positive NICS<sub>zz</sub>(1) of  $+12.4$  ppm, which contradicts the  $\pi$  scheme of the CMO and AdNDP analyses.

One observation in the AdNDP pattern of  $C_{5v} B_{30}$  (**1**) is that, in contrast to the outer  $\pi$  system with ONs of 1.93–1.99 |e|, the inner 15c-2e  $\pi$  sextet has smaller ONs of 1.74–1.82 |e| (Fig. 2(a), second row). The values are not optimal, hinting that the inner  $\pi$  sextet may be more expanded beyond 15 centers. Nonetheless, an ideal AdNDP scheme seems difficult to achieve. Natural charges from NBO analysis of **1** help elucidate the issue from a different angle. As shown in Fig. S2(a) (ESI<sup>†</sup>), there appear to be intramolecular charge transfers in **1**, in particular within the five apex rhombic units in the outer B ribbon, whose B centers carry a charge of  $+0.18$ ,  $-0.05$ , and  $-0.06$  |e|. However, the charge transfers occur only locally and marginally, suggesting that the global bonding in **1** is quite covalent.

The bonding covalency in **1** also helps revisit the bonding nature in corannulene. The knowledge over the past decades is the “annulene-within-an-annulene” model for corannulene, in which not only the rim but also the hub satisfies the  $(4n + 2)$  Hückel rule for aromaticity due to the transfer of one electron from the rim to the central pentagon,<sup>65,66</sup> resulting in an inner cyclopentadienyl anion and an outer [15]annulene cation as mentioned above. Unfortunately, the NBO analysis shows that all the hub and spoke C centers are practically charge neutral ( $-0.01$  and  $-0.05 |e|$ ; Fig. S2(b), ESI†); the main charge transfers are local within the C–H bonds, which do not participate in the  $\pi$

bonding. To be precise, the  $C_5$  hub carries a total negative charge as small as  $-0.05 |e|$ , which is insufficient to fulfill the electron counting of the inner  $\pi$  sextet as a “cyclopentadienyl anion”.

So, the charge-transfer model of corannulene is inconsistent with the NBO charges. Alternatively, the bonding in corannulene should be described as concentric dual  $\pi$  aromaticity, where the  $C_5$  hub manages to gain one extra charge *via* the five spokes by expanding the inner  $\pi$  sextet from  $5c-2e$  to  $10c-2e$   $\pi$  bonds, as illustrated in Fig. 4(b). Indeed, when assumed as  $5c-2e$  bonds, the total ON values in AdNDP for the three inner  $\pi$  bonds amount to  $4.64 |e|$  (Fig. 4(a)), consistent with  $5\pi$  electrons only; whereas the expansion to  $10c-2e$  bonds allows the total ONs to be  $5.90 |e|$  (Fig. 4(b)), perfect for a  $\pi$  sextet. This latter bonding model is entirely covalent in nature and does not require a charge transfer from the outer rim to the inner pentagon, which should be considered as an update of the existing knowledge.<sup>53,66</sup>

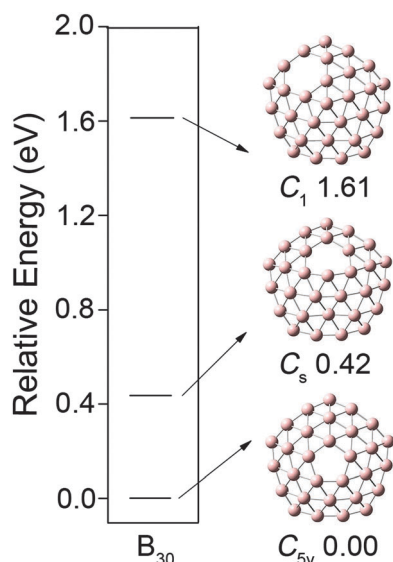


Fig. 5 Energetics for three representative isomeric structures of the  $B_{30}$  cluster, which differ in the position of the hole. At the PBE0/6-311+G(d) level, the  $C_1$  and  $C_s$  isomers are 1.61 and 0.42 eV above the  $C_{5v}$   $B_{30}$  (**1**,  ${}^1A_1$ ) global minimum, respectively.

### 3.4. Why is the pentagonal hole positioned in the center of the bowl-like $B_{30}$ cluster?

The  $B_{30}$  (**1**,  $C_{5v}$ ,  ${}^1A_1$ ) cluster is remarkably symmetric. One question remains to be answered: why is the pentagonal hole situated at the bowl center? To address this question, we made an effort to locate two additional isomeric structures:  $C_s$  and  $C_1$  (Fig. 5). These structures differ from  $C_{5v}$   $B_{30}$  (**1**) in two aspects. First, the hole is moved from the bowl center to the first B ring in  $C_s$  and the second B ring in  $C_1$ . Second, the hole becomes a hexagon in  $C_s$  and  $C_1$ . Intriguingly and not surprisingly, the  $B_{30}$  cluster elevates in energy successively upon moving the hole from the center out: 0.42 eV for  $C_s$  and 1.61 eV for  $C_1$  at the PBE0/6-311+G(d) level. Analogous higher energy structures cannot be located exactly for corannulene, because a B–B link is not equivalent to a C–C one, rather a rhombic  $B_4$  (and to a less extent,  $B_3$  or  $B_5$ ) unit is.<sup>32</sup>

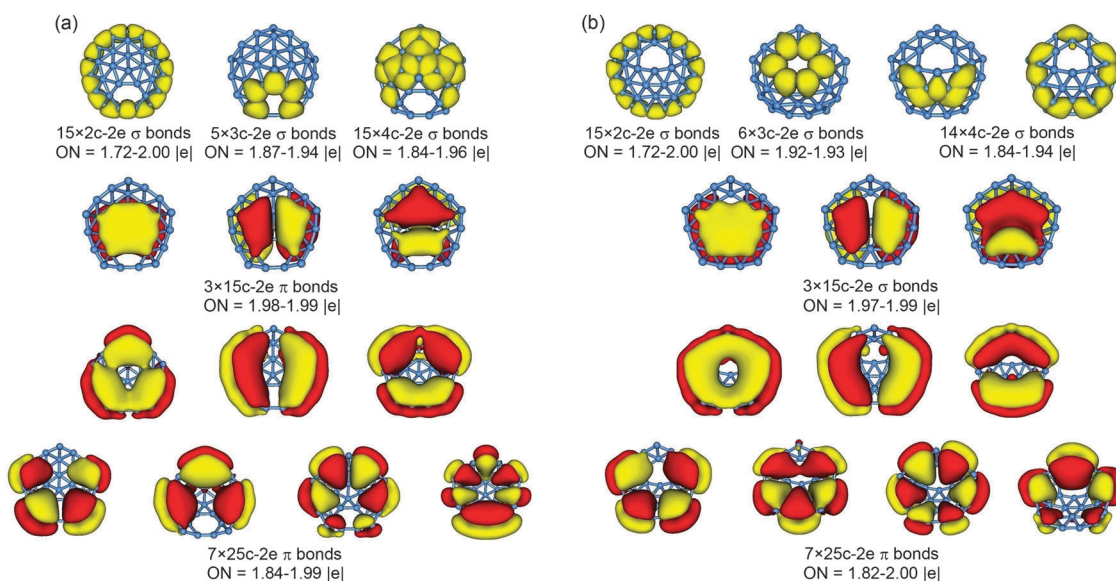


Fig. 6 The adaptive natural density partitioning (AdNDP) bonding patterns for the two higher energy isomers of (a)  $C_1$   $B_{30}$  and (b)  $C_s$   $B_{30}$ . Occupation numbers (ONs) are indicated.

To figure out the mechanism behind the energetics, we analyzed the  $\pi$  CMOs of  $C_s$  and  $C_1$  structures, as shown in Fig. S3 (ESI $\dagger$ ). There are 10  $\pi$  CMOs for each structure, which turn out to exhibit one-to-one correspondence with those of  $C_{5v}$   $B_{30}$  (**1**) and corannulene. Such similarity is independently confirmed from the AdNDP data (Fig. 6). Therefore, the general CMO and AdNDP patterns do not help differentiate between the  $C_{5v}$ ,  $C_s$ , and  $C_1$  isomers. Notably, the center of the inner  $6\pi$  and the outer  $14\pi$  systems points consistently to the bowl center, rather than shifting with the pentagonal/hexagonal hole.

In contrast, the position of the hole markedly alters the energies of individual CMOs. Comparing the  $C_{5v}$  (**1**) and  $C_1$  isomers, for example, the HOMO, HOMO–8, and HOMO–18 orbitals in  $C_1$  (Fig. S3(a), ESI $\dagger$ ) are energetically destabilized by 0.60, 0.54, and 0.46 eV, respectively, relative to HOMO', HOMO–5', and HOMO–12' in  $C_{5v}$  (**1**) (Fig. S1(a), ESI $\dagger$ ). For these CMOs, the electron cloud covers the hole extensively in  $C_1$ , which effectively destabilizes them. We believe that the central hole in  $C_{5v}$  (**1**) is advantageous and can lead to an overall stabilization with respect to the  $C_s$  and  $C_1$  isomers, presumably because the number of CMOs that cloud over the central hole ( $C_{5v}$ ; Fig. S1(a), ESI $\dagger$ ) is substantially smaller than that on an off-center hole ( $C_s$  or  $C_1$ ; Fig. S3, ESI $\dagger$ ). In other words, the defective hole in  $C_{5v}$  (**1**) destabilizes the smallest number of CMOs energetically, making it the most stable species.

### 3.5. Simulated infrared spectra of $C_{5v}$ $B_{30}$ (**1**) and $C_{20}H_{10}$ (**2**)

We have calculated the vibrational properties of  $C_{5v}$   $B_{30}$  (**1**) at the PBE0/6-311G(d) level, simulated its infrared (IR) spectrum, and compared them with  $C_{20}H_{10}$  (**2**). The simulated IR spectra are presented in Fig. 7. An intense peak at  $3202\text{ cm}^{-1}$  in **2** corresponds to the characteristic asymmetric stretching of C–H bonds. The intense IR peak situated at  $856\text{ cm}^{-1}$  in **2** is the out-of-plane bending of C–H terminals, whose corresponding B–B bending mode in **1** turns out to be weak and appears at  $488\text{ cm}^{-1}$ . The asymmetric B–B stretching vibrations in **1** produce two

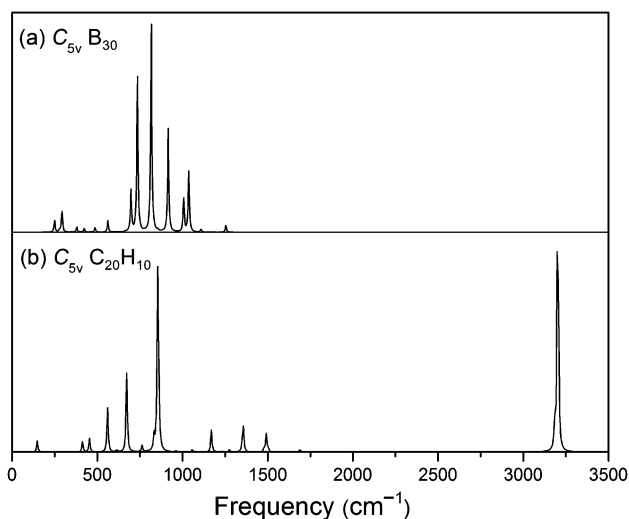


Fig. 7 Predicted infrared spectra of (a)  $C_{5v}$   $B_{30}$  (**1**,  $^1A_1$ ) and (b)  $C_{20}H_{10}$  (**2**,  $^1A_1$ ) at the PBE0/6-311+G(d) level.

degenerate IR bands at  $817\text{ cm}^{-1}$ , whereas the in-plane bending B–B modes correspond to two degenerate IR absorption bands at  $736\text{ cm}^{-1}$ . All other IR active modes in **1** are very weak. The predicted IR spectrum should aid forthcoming experimental characterization of  $C_{5v}$   $B_{30}$  (**1**).

## 4. Conclusions

We have computationally studied the chemical bonding in a quasi-planar, bowl-like  $B_{30}$  (**1**,  $C_{5v}$ ,  $^1A_1$ ) cluster, which consists of two circular B double-chain ribbons and possesses a concentric dual  $\pi$  aromatic system. The inner and outer B ribbons in  $B_{30}$  support  $6\pi$  and  $14\pi$  electrons, respectively, conforming to the  $(4n + 2)$  Hückel rule. The bonding model is established from concerted quantum chemical data based on canonical molecular orbital analysis, adaptive natural density partitioning, nucleus-independent chemical shifts, and natural charge calculations. The bowl-like  $B_{30}$  cluster is shown to be an all-boron analogue of corannulene  $C_{20}H_{10}$  (**2**,  $C_{5v}$ ,  $^1A_1$ ), and the bonding nature of the latter is revisited and fully elucidated. The  $C_{5v}$   $B_{30}$  cluster is compared with two alternative structural isomers ( $C_s$  and  $C_1$ ), unraveling the mechanism why the defective hole prefers to be positioned at the bowl center.

## Acknowledgements

This work was supported by the National Natural Science Foundation of China (21573138), the State Key Laboratory of Quantum Optics and Quantum Optics Devices (KF201402), and the Natural Science Foundation of Shandong Province (ZR2014BL011).

## References

- 1 I. Boustani, *Phys. Rev. B: Condens. Matter Mater. Phys.*, 1997, **55**, 16426.
- 2 J. I. Aihara, H. Kanno and T. Ishida, *J. Am. Chem. Soc.*, 2005, **127**, 13324.
- 3 E. Oger, N. R. M. Crawford, R. Kelting, P. Weis, M. M. Kappes and R. Ahlrichs, *Angew. Chem., Int. Ed.*, 2007, **46**, 8503.
- 4 J. E. Fowler and J. M. Ugalde, *J. Phys. Chem. A*, 2000, **104**, 397.
- 5 H. J. Zhai, B. Kiran, J. Li and L. S. Wang, *Nat. Mater.*, 2003, **2**, 827.
- 6 A. N. Alexandrova, A. I. Boldyrev, H. J. Zhai and L. S. Wang, *Coord. Chem. Rev.*, 2006, **250**, 2811.
- 7 H. J. Zhai, L. S. Wang, A. N. Alexandrova and A. I. Boldyrev, *J. Phys. Chem. A*, 2003, **107**, 9319.
- 8 H. J. Zhai, L. S. Wang, A. N. Alexandrova and A. I. Boldyrev, *J. Chem. Phys.*, 2002, **117**, 7917.
- 9 A. N. Alexandrova, A. I. Boldyrev, H. J. Zhai, L. S. Wang, E. Steiner and P. W. Fowler, *J. Phys. Chem. A*, 2003, **107**, 1359.
- 10 A. N. Alexandrova, A. I. Boldyrev, H. J. Zhai and L. S. Wang, *J. Chem. Phys.*, 2005, **122**, 054313.
- 11 A. N. Alexandrova, A. I. Boldyrev, H. J. Zhai and L. S. Wang, *J. Phys. Chem. A*, 2004, **108**, 3509.
- 12 H. J. Zhai, A. N. Alexandrova, K. A. Birch, A. I. Boldyrev and L. S. Wang, *Angew. Chem., Int. Ed.*, 2003, **42**, 6004.

- 13 A. N. Alexandrova, H. J. Zhai, L. S. Wang and A. I. Boldyrev, *Inorg. Chem.*, 2004, **43**, 3552.
- 14 A. P. Sergeeva, D. Yu. Zubarev, H. J. Zhai, A. I. Boldyrev and L. S. Wang, *J. Am. Chem. Soc.*, 2008, **130**, 7244.
- 15 C. Romanescu, D. J. Harding, A. Fielicke and L. S. Wang, *J. Chem. Phys.*, 2012, **137**, 014317.
- 16 W. Huang, A. P. Sergeeva, H. J. Zhai, B. B. Averkiev, L. S. Wang and A. I. Boldyrev, *Nat. Chem.*, 2010, **2**, 202.
- 17 B. Kiran, S. Bulusu, H. J. Zhai, S. Yoo, X. C. Zeng and L. S. Wang, *Proc. Natl. Acad. Sci. U. S. A.*, 2005, **102**, 961.
- 18 Z. A. Piazza, W. L. Li, C. Romanescu, A. P. Sergeeva, L. S. Wang and A. I. Boldyrev, *J. Chem. Phys.*, 2012, **136**, 104310.
- 19 A. P. Sergeeva, Z. A. Piazza, C. Romanescu, W. L. Li, A. I. Boldyrev and L. S. Wang, *J. Am. Chem. Soc.*, 2012, **134**, 18065.
- 20 I. A. Popov, Z. A. Piazza, W. L. Li, L. S. Wang and A. I. Boldyrev, *J. Chem. Phys.*, 2013, **139**, 144307.
- 21 Z. A. Piazza, I. A. Popov, W. L. Li, R. Pal, X. C. Zeng, A. I. Boldyrev and L. S. Wang, *J. Chem. Phys.*, 2014, **141**, 034303.
- 22 W. L. Li, Y. F. Zhao, H. S. Hu, J. Li and L. S. Wang, *Angew. Chem., Int. Ed.*, 2014, **53**, 5540.
- 23 I. Boustani, A. Rubio and J. A. Alonso, *Chem. Phys. Lett.*, 1999, **311**, 21.
- 24 W. L. Li, Q. Chen, W. J. Tian, H. Bai, Y. F. Zhao, H. S. Hu, J. Li, H. J. Zhai, S. D. Li and L. S. Wang, *J. Am. Chem. Soc.*, 2014, **136**, 12257.
- 25 Z. A. Piazza, H. S. Hu, W. L. Li, Y. F. Zhao, J. Li and L. S. Wang, *Nat. Commun.*, 2014, **5**, 3113.
- 26 Q. Chen, G. F. Wei, W. J. Tian, H. Bai, Z. P. Liu, H. J. Zhai and S. D. Li, *Phys. Chem. Chem. Phys.*, 2014, **16**, 18282.
- 27 H. J. Zhai, Y. F. Zhao, W. L. Li, Q. Chen, H. Bai, H. S. Hu, Z. A. Piazza, W. J. Tian, H. G. Lu, Y. B. Wu, Y. W. Mu, G. F. Wei, Z. P. Liu, J. Li, S. D. Li and L. S. Wang, *Nat. Chem.*, 2014, **6**, 727.
- 28 Q. Chen, W. L. Li, Y. F. Zhao, S. Y. Zhang, H. S. Hu, H. Bai, H. R. Li, W. J. Tian, H. G. Lu, H. J. Zhai, S. D. Li, J. Li and L. S. Wang, *ACS Nano*, 2015, **9**, 754.
- 29 Q. Chen, S. Y. Zhang, H. Bai, W. J. Tian, T. Gao, H. R. Li, C. Q. Miao, Y. W. Mu, H. G. Lu, H. J. Zhai and S. D. Li, *Angew. Chem., Int. Ed.*, 2015, **54**, 8160.
- 30 Y. J. Wang, Y. F. Zhao, W. L. Li, T. Jian, Q. Chen, X. R. You, T. Ou, X. Y. Zhao, H. J. Zhai, S. D. Li, J. Li and L. S. Wang, *J. Chem. Phys.*, 2016, **144**, 064307.
- 31 D. Z. Li, H. Bai, Q. Chen, H. G. Lu, H. J. Zhai and S. D. Li, *J. Chem. Phys.*, 2013, **138**, 244304.
- 32 H. J. Zhai, Q. Chen, H. Bai, S. D. Li and L. S. Wang, *Acc. Chem. Res.*, 2014, **47**, 2435.
- 33 H. J. Zhai, L. M. Wang, S. D. Li and L. S. Wang, *J. Phys. Chem. A*, 2007, **111**, 1030.
- 34 H. J. Zhai, S. D. Li and L. S. Wang, *J. Am. Chem. Soc.*, 2007, **129**, 9254.
- 35 S. D. Li, H. J. Zhai and L. S. Wang, *J. Am. Chem. Soc.*, 2008, **130**, 2573.
- 36 D. Z. Li, H. Bai, T. Ou, Q. Chen, H. J. Zhai and S. D. Li, *J. Chem. Phys.*, 2015, **142**, 014302.
- 37 J. O. C. Jiménez-Halla, R. Islas, T. Heine and G. Merino, *Angew. Chem., Int. Ed.*, 2010, **49**, 5668.
- 38 G. Martínez-Guajardo, A. P. Sergeeva, A. I. Boldyrev, T. Heine, J. M. Ugalde and G. Merino, *Chem. Commun.*, 2011, **47**, 6242.
- 39 Y. J. Wang, X. Y. Zhao, Q. Chen, H. J. Zhai and S. D. Li, *Nanoscale*, 2015, **7**, 16054.
- 40 Y. J. Wang, X. R. You, Q. Chen, L. Y. Feng, K. Wang, T. Ou, X. Y. Zhao, H. J. Zhai and S. D. Li, *Phys. Chem. Chem. Phys.*, 2016, **18**, 15774.
- 41 T. B. Tai, L. V. Duong, H. T. Pham, D. T. T. Mai and M. T. Nguyen, *Chem. Commun.*, 2014, **50**, 1558.
- 42 C. Adamo and V. Barone, *J. Chem. Phys.*, 1999, **110**, 6158.
- 43 J. P. Perdew, K. Burke and M. Ernzerhof, *Phys. Rev. Lett.*, 1996, **77**, 3865.
- 44 J. P. Perdew, K. Burke and M. Ernzerhof, *Phys. Rev. Lett.*, 1997, **78**, 1396.
- 45 R. Krishnan, J. S. Binkley, R. Seeger and J. A. Pople, *J. Chem. Phys.*, 1980, **72**, 650.
- 46 F. Y. Li, P. Jin, D. E. Jiang, L. Wang, S. B. B. Zhang, J. J. Zhao and Z. F. Chen, *J. Chem. Phys.*, 2012, **136**, 074302.
- 47 H. Bai, Q. Chen, C. Q. Miao, Y. W. Mu, Y. B. Wu, H. G. Lu, H. J. Zhai and S. D. Li, *Phys. Chem. Chem. Phys.*, 2013, **15**, 18872.
- 48 D. Yu. Zubarev and A. I. Boldyrev, *Phys. Chem. Chem. Phys.*, 2008, **10**, 5207.
- 49 P. v. R. Schleyer, C. Maerker, A. Dransfeld, H. J. Jiao and N. J. R. V. E. Hommes, *J. Am. Chem. Soc.*, 1996, **118**, 6317.
- 50 E. D. Glendening, J. K. Badenhoop, A. E. Reed, J. E. Carpenter, J. A. Bohmann, C. M. Morales and F. Weinhold, *NBO 5.0*, Theoretical Chemistry Institute, University of Wisconsin, Madison, 2001.
- 51 M. J. Frisch, *et al.*, Gaussian 09, revision D.01, Gaussian, Inc., Wallingford, CT, 2009.
- 52 U. Varetto, *Molekel 5.4.0.8*, Swiss National Supercomputing Center, Manno, Switzerland, 2009.
- 53 W. E. Barth and R. G. Lawton, *J. Am. Chem. Soc.*, 1966, **88**, 380.
- 54 L. Hedberg, K. Hedberg, P. C. Cheng and L. T. Scott, *J. Phys. Chem. A*, 2000, **104**, 7689.
- 55 W. C. Herndon, *J. Am. Chem. Soc.*, 1974, **96**, 7605.
- 56 P. Pykkö and M. Atsumi, *Chem. – Eur. J.*, 2009, **15**, 12770.
- 57 P. Pykkö, *J. Phys. Chem. A*, 2015, **119**, 2326.
- 58 D. Jose and A. Datta, *J. Phys. Chem. C*, 2012, **116**, 24639.
- 59 T. K. Mandal, D. Jose, A. Nijamudheen and A. Datta, *J. Phys. Chem. C*, 2014, **118**, 12115.
- 60 B<sub>30</sub> (**1**, C<sub>5v</sub>) and corannulene C<sub>20</sub>H<sub>10</sub> (**2**, C<sub>5v</sub>) have exactly the same number of 90 valence electrons, which are divided into two subsets: 20π electrons versus 70σ electrons. A comparison to demonstrate the one-to-one correspondence of all σ canonical molecular orbitals (CMOs) between the two systems does not appear feasible and necessary. Instead, the AdNDP data (Fig. 2), which are equivalent to the CMOs, are easier and more straightforward to follow. The first row in Fig. 2(b) shows the 35 σ CMOs of **2**, including (i) 10 C–H and 5 rim σ bonds, (ii) 5 hub σ bonds, (iii) 5 spoke σ bonds, and (iv) 10 flank σ bonds. Approximately, these are comparable to the σ bonds of **1**; see Fig. 2(a), first row, from left to right. We note that it is conceptually known that a B<sub>4</sub> (and to a less extent, B<sub>3</sub> or B<sub>5</sub>) unit in boron clusters

- can be equivalent to a C–C unit in hydrocarbons in terms of bonding.<sup>32</sup>
- 61 The AdNDP  $\sigma$  scheme in Fig. 2(a) is uniform for spatial coverage of twenty 3c-2e/4c-2e  $\sigma$  bonds over the bowl, except for one triangular hole along each edge on the third B ring. Technically, this can be compensated for by expansion of five peripheral  $\sigma$  bonds from 2c-2e to 3c-2e. Nonetheless, it does not make any fundamental difference in terms of the nature of bonding in the  $\sigma$  framework.
- 62 D. Z. Li, Q. Chen, Y. B. Wu, H. G. Lu and S. D. Li, *Phys. Chem. Chem. Phys.*, 2012, **14**, 14769.
- 63 H. J. Zhai, Q. Chen, H. Bai, H. G. Lu, W. L. Li, S. D. Li and L. S. Wang, *J. Chem. Phys.*, 2013, **139**, 174301.
- 64 P. Lazzeretti, *Phys. Chem. Chem. Phys.*, 2004, **6**, 217.
- 65 W. E. Barth and R. G. Lawton, *J. Am. Chem. Soc.*, 1971, **93**, 1730.
- 66 G. Monaco, L. T. Scott and R. Zanasi, *J. Phys. Chem. A*, 2008, **112**, 8136.